Measurement of Single Electrons and Implications for Charm Production in Au + Au Collisions at $\sqrt{s_{NN}} = 130$ GeV

K. Adcox,[40] S. S. Adler,[3] N. N. Ajitanand,[27] Y. Akiba,[14] J. Alexander,[27] L. Aphecetche,[34] Y. Arai,[14] S. H. Aronson,[3] R. Averbeck,[28] T. C. Awes,[29] K. N. Barish,[5] P. D. Barnes,[19] J. Barrette,[21] B. Bassalleck,[25] S. Bathe,[22] V. Baublis,[30] A. Bazilevsky,[12,32] S. Belikov,[12,13] F. G. Bellaiche,[29] S. T. Belyaev,[16] M. J. Bennett,[19] Y. Berdnikov,[35] S. Botelho,[33] M. L. Brooks,[19] D. S. Brown,[26] N. Bruner,[25] D. Bucher,[22] H. Buesching,[22] V. Bumazhnov,[12] G. Bunce,[3,32] J. Burward-Hoy,[28] S. Butsyk,[28,30] T. A. Carey,[19] P. Chand,[2] J. Chang,[5] W. C. Chang,[1] L. L. Chavez,[25] S. Chernichenko,[12] C. Y. Chi,[8] J. Chiba,[14] M. Chiu,[8] R. K. Choudhury,[2] T. Christ,[28] T. Chujo,[3,39] M. S. Chung,[15,19] P. Chung,[27] V. Cianciolo,[29] B. A. Cole,[8] D. G. D'Enterria,[34] G. David,[3] H. Delagrange,[34] A. Denisov,[12] A. Deshpande,[32] E. J. Desmond,[3] O. Dietzsch,[33] B. V. Dinesh,[2] A. Drees,[28] A. Durum,[12] D. Dutta,[2] K. Ebisu,[24] Y. V. Efremenko,[29] K. El Chenawi,[40] H. En'yo,[17,31] S. Esumi,[39] L. Ewell,[3] T. Ferdousi,[5] D. E. Fields,[25] S. L. Fokin,[16] Z. Fraenkel,[42] A. Franz,[3] A. D. Frawley,[9] S.-Y. Fung,[5] S. Garpman,[20,*] T. K. Ghosh,[40] A. Glenn,[36] A. L. Godoi,[33] Y. Goto,[32] S. V. Greene,[40] M. Grosse Perdekamp,[32] S. K. Gupta,[2] W. Guryn,[3] H.-Å. Gustafsson,[20] T. Hachiya,[11] J. S. Haggerty,[3] H. Hamagaki,[7] A. G. Hansen,[19] H. Hara,[24] E. P. Hartouni,[18] R. Hayano,[38] N. Hayashi,[31] X. He,[10] T. K. Hemmick,[28] J. M. Heuser,[28] M. Hibino,[41] J. C. Hill,[13] D. S. Ho,[43] K. Homma,[11] B. Hong,[15] A. Hoover,[26] T. Ichihara,[31,32] K. Imai,[17,31] M. S. Ippolitov,[16] M. Ishihara,[31,32] B. V. Jacak,[28,32] W. Y. Jang,[15] J. Jia,[28] B. M. Johnson,[3] S. C. Johnson,[18,28] K. S. Joo,[23] S. Kametani,[41] J. H. Kang,[43] M. Kann,[30] S. S. Kapoor,[2] S. Kelly,[8] B. Khachaturov,[42] A. Khanzadeev,[30] J. Kikuchi,[41] D. J. Kim,[43] H. J. Kim,[43] S. Y. Kim,[43] Y. G. Kim,[43] W. W. Kinnison,[19] E. Kistenev,[3] A. Kiyomichi,[39] C. Klein-Boesing,[22] S. Klinksiek,[25] L. Kochenda,[30] V. Kochetkov,[12] D. Koehler,[25] T. Kohama,[11] D. Kotchetkov,[5] A. Kozlov,[42] P. J. Kroon,[3] K. Kurita,[31,32] M. J. Kweon,[15] Y. Kwon,[43] G. S. Kyle,[26] R. Lacey,[27] J. G. Lajoie,[13] J. Lauret,[27] A. Lebedev,[13,16] D. M. Lee,[19] M. J. Leitch,[19] X. H. Li,[5] Z. Li,[6,31] D. J. Lim,[43] M. X. Liu,[19] X. Liu,[6] Z. Liu,[6] C. F. Maguire,[40] J. Mahon,[3] Y. I. Makdisi,[3] V. I. Manko,[16] Y. Mao,[6,31] S. K. Mark,[21] S. Markacs,[8] G. Martinez,[34] M. D. Marx,[28] A. Masaike,[17] F. Matathias,[28] T. Matsumoto,[7,41] P. L. McGaughey,[19] E. Melnikov,[12] M. Merschmeyer,[22] F. Messer,[28] M. Messer,[3] Y. Miake,[39] T. E. Miller,[40] A. Milov,[42] S. Mioduszewski,[3,36] R. E. Mischke,[19] G. C. Mishra,[10] J. T. Mitchell,[3] A. K. Mohanty,[2] D. P. Morrison,[3] J. M. Moss,[19] F. Mühlbacher,[28] M. Muniruzzaman,[5] J. Murata,[31] S. Nagamiya,[14] Y. Nagasaka,[24] J. L. Nagle,[8] Y. Nakada,[17] B. K. Nandi,[5] J. Newby,[36] L. Nikkinen,[21] P. Nilsson,[20] S. Nishimura,[7] A. S. Nyanin,[16] J. Nystrand,[20] E. O'Brien,[3] C. A. Ogilvie,[13] H. Ohnishi,[3,11] I. D. Ojha,[4,40] M. Ono,[39] V. Onuchin,[12] A. Oskarsson,[20] L. Österman,[20] I. Otterlund,[20] K. Oyama,[7,38] L. Paffrath,[3,*] A. P. T. Palounek,[19] V. S. Pantuev,[28] V. Papavassiliou,[26] S. F. Pate,[26] T. Peitzmann,[22] A. N. Petridis,[13] C. Pinkenburg,[3,27] R. P. Pisani,[3] P. Pitukhin,[12] F. Plasil,[29] M. Pollack,[28,36] K. Pope,[36] M. L. Purschke,[3] I. Ravinovich,[42] K. F. Read,[29,36] K. Reygers,[22] V. Riabov,[30,35] Y. Riabov,[30] M. Rosati,[13] A. A. Rose,[40] S. S. Ryu,[43] N. Saito,[31,32] A. Sakaguchi,[11] T. Sakaguchi,[7,41] H. Sako,[39] T. Sakuma,[31,37] V. Samsonov,[30] T. C. Sangster,[18] R. Santo,[22] H. D. Sato,[17,31] S. Sato,[39] S. Sawada,[14] B. R. Schlei,[19] Y. Schutz,[34] V. Semenov,[12] R. Seto,[5] T. K. Shea,[3] I. Shein,[12] T.-A. Shibata,[31,37] K. Shigaki,[14] T. Shiina,[19] Y. H. Shin,[43] I. G. Sibiriak,[16] D. Silvermyr,[20] K. S. Sim,[15] J. Simon-Gillo,[19] C. P. Singh,[4] V. Singh,[4] M. Sivertz,[3] A. Soldatov,[12] R. A. Soltz,[18] S. Sorensen,[29,36] P. W. Stankus,[29] N. Starinsky,[21] P. Steinberg,[8] E. Stenlund,[20] A. Ster,[44] S. P. Stoll,[3] M. Sugioka,[31,37] T. Sugitate,[11] J. P. Sullivan,[19] Y. Sumi,[11] Z. Sun,[6] M. Suzuki,[39] E. M. Takagui,[33] A. Taketani,[31] M. Tamai,[41] K. H. Tanaka,[14] Y. Tanaka,[24] E. Taniguchi,[31,37] M. J. Tannenbaum,[3] J. Thomas,[28] J. H. Thomas,[18] T. L. Thomas,[25] W. Tian,[6,36] J. Tojo,[17,31] H. Torii,[17,31] R. S. Towell,[19] I. Tserruya,[42] H. Tsuruoka,[39] A. A. Tsvetkov,[16] S. K. Tuli,[4] H. Tydesjö,[20] N. Tyurin,[12] T. Ushiroda,[24] H. W. van Hecke,[19] C. Velissaris,[26] J. Velkovska,[28] M. Velkovsky,[28] A. A. Vinogradov,[16] M. A. Volkov,[16] A. Vorobyov,[30] E. Vznuzdaev,[30] H. Wang,[5] Y. Watanabe,[31,32] S. N. White,[3] C. Witzig,[3] F. K. Wohn,[13] C. L. Woody,[3] W. Xie,[5,42] K. Yagi,[39] S. Yokkaichi,[31] G. R. Young,[29] I. E. Yushmanov,[16] W. A. Zajc,[8] Z. Zhang,[28] and S. Zhou[6]

(PHENIX Collaboration)

[1]*Institute of Physics, Academia Sinica, Taipei 11529, Taiwan*
[2]*Bhabha Atomic Research Centre, Bombay 400 085, India*
[3]*Brookhaven National Laboratory, Upton, New York 11973-5000*
[4]*Department of Physics, Banaras Hindu University, Varanasi 221005, India*
[5]*University of California–Riverside, Riverside, California 92521*
[6]*China Institute of Atomic Energy (CIAE), Beijing, People's Republic of China*
[7]*Center for Nuclear Study, Graduate School of Science, University of Tokyo, 7-3-1 Hongo, Bunkyo, Tokyo 113-0033, Japan*

[8]Columbia University, New York, New York 10027
and Nevis Laboratories, Irvington, New York 10533
[9]Florida State University, Tallahassee, Florida 32306
[10]Georgia State University, Atlanta, Georgia 30303
[11]Hiroshima University, Kagamiyama, Higashi-Hiroshima 739-8526, Japan
[12]Institute for High Energy Physics (IHEP), Protvino, Russia
[13]Iowa State University, Ames, Iowa 50011
[14]KEK, High Energy Accelerator Research Organization, Tsukuba-shi, Ibaraki-ken 305-0801, Japan
[15]Korea University, Seoul, 136-701, Korea
[16]Russian Research Center "Kurchatov Institute," Moscow, Russia
[17]Kyoto University, Kyoto 606, Japan
[18]Lawrence Livermore National Laboratory, Livermore, California 94550
[19]Los Alamos National Laboratory, Los Alamos, New Mexico 87545
[20]Department of Physics, Lund University, Box 118, SE-221 00 Lund, Sweden
[21]McGill University, Montreal, Quebec, Canada H3A 2T8
[22]Institut für Kernphysik, University of Münster, D-48149 Münster, Germany
[23]Myongji University, Yongin, Kyonggido 449-728, Korea
[24]Nagasaki Institute of Applied Science, Nagasaki-shi, Nagasaki 851-0193, Japan
[25]University of New Mexico, Albuquerque, New Mexico 87131
[26]New Mexico State University, Las Cruces, New Mexico 88003
[27]Chemistry Department, State University of New York–Stony Brook, Stony Brook, New York 11794
[28]Department of Physics and Astronomy, State University of New York–Stony Brook, Stony Brook, New York 11794
[29]Oak Ridge National Laboratory, Oak Ridge, Tennessee 37831
[30]PNPI, Petersburg Nuclear Physics Institute, Gatchina, Russia
[31]RIKEN (The Institute of Physical and Chemical Research), Wako, Saitama 351-0198, Japan
[32]RIKEN BNL Research Center, Brookhaven National Laboratory, Upton, New York 11973-5000
[33]Universidade de São Paulo, Instituto de Física, Caixa Postal 66318, São Paulo CEP05315-970, Brazil
[34]SUBATECH (Ecole des Mines de Nantes, INP3/CNRS, Universite de Nantes), BP 20722-44307, Nantes-Cedex 3, France
[35]St. Petersburg State Technical University, St. Petersburg, Russia
[36]University of Tennessee, Knoxville, Tennessee 37996
[37]Department of Physics, Tokyo Institute of Technology, Tokyo, 152-8551, Japan
[38]University of Tokyo, Tokyo, Japan
[39]Institute of Physics, University of Tsukuba, Tsukuba, Ibaraki 305, Japan
[40]Vanderbilt University, Nashville, Tennessee 37235
[41]Waseda University, Advanced Research Institute for Science and Engineering, 17 Kikui-cho, Shinjuku-ku, Tokyo 162-0044, Japan
[42]Weizmann Institute, Rehovot 76100, Israel
[43]Yonsei University, IPAP, Seoul 120-749, Korea
[44]KFKI Research Institute for Particle and Nuclear Physics (RMKI), Budapest, Hungary[†]

Transverse momentum spectra of electrons from Au + Au collisions at $\sqrt{s_{NN}} = 130$ GeV have been measured at midrapidity by the PHENIX experiment at the Relativistic Heavy Ion Collider. The spectra show an excess above the background from photon conversions and light hadron decays. The electron signal is consistent with that expected from semileptonic decays of charm. The yield of the electron signal dN_e/dy for $p_T > 0.8$ GeV/c is 0.025 ± 0.004(stat) ± 0.010(syst) in central collisions, and the corresponding charm cross section is 380 ± 60(stat) ± 200(syst) μb per binary nucleon-nucleon collision.

In this Letter, we report the first measurement of single electron spectra, $(e^+ + e^-)/2$, in Au + Au collisions at $\sqrt{s_{NN}} = 130$ GeV at the Relativistic Heavy Ion Collider (RHIC). The measurement of single leptons at high transverse momentum ($p_T \gtrsim 1$ GeV/c) is a useful way to study heavy-quark production, an important probe of hot and dense matter created in high energy heavy ion collisions. Charm production is sensitive to the initial state gluon density [1,2]. Nuclear and medium effects, such as shadowing and charm quark energy loss [3,4], can be studied by comparison of charm production in AA, pA, and pp collisions. Measurement of charm is important

for understanding J/ψ suppression (a proposed signal of the deconfinement phase transition [5,6]) and the dilepton mass distribution in $1 < M_{l^+l^-} < 3$ GeV, where lepton pairs from charm make significant contributions [7]. In pp collisions at the CERN Intersecting Storage Rings (ISR) ($\sqrt{s} = 30$–63 GeV), production of single electrons was observed ($e/\pi \sim 10^{-4}$) for $p_T > 1$ GeV/c [8–11], and interpreted as evidence of open charm production [12]. In pp collisions at RHIC energies, the signal level is expected to be higher, since charm production increases with $\sqrt{s_{NN}}$ faster than pion production. We recently observed suppression of high p_T pion production in Au + Au collisions at

RHIC relative to binary nucleon-nucleon (*NN*) collision scaling [13]. If charm production scales with *NN* collisions, as expected in the absence of nuclear effects, the e/π ratio will be even higher in Au + Au collisions at RHIC.

Data used for this analysis were recorded by the PHENIX west-arm spectrometer [14] ($\Delta\phi = 90°$ in azimuth, $|\eta| < 0.35$ in pseudorapidity), which consisted of a drift chamber (DC), a layer of pad chambers (PC1), a ring imaging Čerenkov detector (RICH), and a lead-scintillator electromagnetic calorimeter (EMCAL). The trigger was provided by beam-beam counters (BBC) and zero-degree calorimeters (ZDC). ZDC and BBC signals were combined to select centrality: central (0%–10%), peripheral (60%–80%), and minimum bias (0%–92%) [15].

The analysis uses $1.23M$ minimum bias events with vertex position $|z| < 30$ cm. Charged particle tracks are reconstructed by the DC and the PC1 with a momentum resolution $\delta p / p \simeq 0.6\% \oplus 3.6\% \, p$ (GeV/c). Tracks are confirmed by a matching hit in the EMCAL, which measures the energy E deposited with a resolution of $8.2\%/\sqrt{E(\text{GeV})} \oplus 1.9\%$ for test beam electrons. Electron identification is performed using the RICH and the EMCAL [14]. The RICH is filled with 1 atm CO_2 and detects on average 10.8 photoelectrons per electron track, while a pion with $p < 4.7$ GeV/c produces no signal. It is required that at least three RICH hits are associated with the track and that their hit pattern is consistent with that of an electron track. After these cuts, a clear electron signal is observed as a narrow peak centered at $E/p = 1.0$. We select tracks in the peak as electron candidates. The E/p cut reduces hadron background and removes conversion electrons created far from the vertex. A hadron deposits only a fraction of its energy in the EMCAL, and the momentum of an off-vertex conversion electron is reconstructed incorrectly. The remaining background, about 10% of the electron candidates, is caused by accidental association of RICH hits with hadron tracks. The background level is measured statistically by an event mixing method, and is subtracted from the yield.

The electron acceptance (~7.4% of dN/dy) and efficiency (~60%) are determined using a detailed GEANT [16] simulation, which satisfactorily reproduces the detector response. Additionally, a multiplicity dependent efficiency loss due to detector occupancy is evaluated by embedding simulated electrons into real events. This efficiency loss is $27 \pm 4\%$ ($4 \pm 2\%$) for central (peripheral) collisions and has no significant p_T dependence.

Figure 1 shows the p_T distributions of electrons in PHENIX for central, minimum bias, and peripheral collisions. Errors in the figure are statistical. The overall systematic uncertainty, which is the quadratic sum of several few percent effects, is about 11%. Expected sources of electrons are (1) Dalitz decays of π^0, η, η', ω, and ϕ, (2) dielectron decays of ρ, ω, and ϕ, (3) photon conversions, (4) kaon decays ($K^{0,\pm} \rightarrow \pi e \nu$),
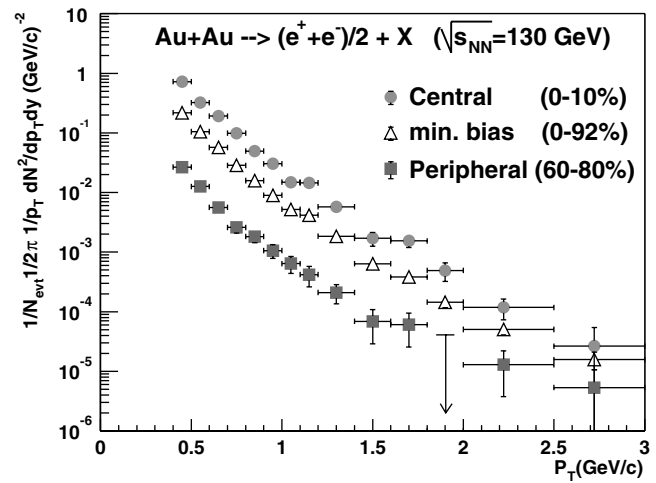

FIG. 1. Transverse momentum spectra of electrons in PHENIX from Au + Au collisions at $\sqrt{s_{NN}} = 130$ GeV.

(5) semileptonic decay of charm, and (6) other contributions such as bottom decays and thermal dileptons. In this analysis, sources (1)–(4) are considered to be background.

We have calculated the contributions from Dalitz and dielectron decays with a hadron decay generator. PHENIX has measured the p_T distributions of $\pi^\pm$ in $0.2 < p_T < 2.2$ GeV/c [17] and of π^0 in $1 < p_T < 4$ GeV/c [13]. Since the $\pi^\pm$ and π^0 data are consistent in the overlapping region, we fit a power law function to the combined data sets to determine the input π^0 spectrum for the decay generator. The p_T distribution of any other hadron h is obtained from the π^0 spectrum by replacing p_T with $\sqrt{p_T^2 + m_h^2 - m_{\pi^0}^2}$. The shapes of the resulting p_T spectra of $K^\pm$, p, and $\bar{p}$ agree with the PHENIX measurements [17] within 20%. In this parametrization h/π^0 ratios approach constants at high p_T. We assume the following asymptotic ratios to fix the relative normalizations: $\eta/\pi^0 = 0.55$, $\eta'/\pi^0 = 0.25$, $\rho/\pi^0 = \omega/\pi^0 = 1.0$, $\phi/\pi^0 = 0.40$. Except for the ϕ, these ratios are taken from proton beam data of CERN Super Proton Synchrotron (SPS), FNAL, and ISR experiments [18,19]. The η/π^0 ratio is consistent with a measurement in Pb + Pb collisions at SPS [20]. The ϕ/π^0 ratio is based on the integrated ratio $\phi/h^- \sim 0.02$ in Au + Au collisions at $\sqrt{s_{NN}} = 130$ GeV [21]. We assign to each ratio a conservative systematic uncertainty of 50%.

Photon conversions are evaluated using a combination of the GEANT simulation and the hadron decay generator. Since p_T spectra of externally converted electrons are similar to those from Dalitz decay, the conversion spectra can be approximated by scaling the Dalitz decay spectra by an experiment specific factor, $R_{\text{conv}} = \text{conversion/Dalitz}$. R_{conv} is evaluated using the GEANT simulation and is cross-checked by comparing the relative yield of reconstructed Dalitz and conversion pairs in the simulation and in the data. The simulation shows that R_{conv} has only a weak p_T dependence, primarily due to the energy dependence

of the pair creation cross section. R_{conv} is parametrized as $(1.9 \pm 0.2) \times (1 - 0.0718 \times p_T^{-0.76})$.

Background from kaon decays is also evaluated using the GEANT simulation and is found to be negligible.

The upper panel of Fig. 2 shows the ratio of the measured electrons to the calculated background versus p_T for minimum bias events. The shaded region is the quadratic sum of systematic errors in the electron measurement and in the background. The latter includes uncertainties in the normalization and the shape of the π^0 spectrum, in the h/π^0 ratios, and in R_{conv}. A significant electron excess above the background is observed for $p_T > 0.6$ GeV/c. Central collisions show a similar excess. The peripheral collision data sample lacks sufficient statistics to reveal a signal in this analysis.

Fractional contributions to the background are shown in the lower panel of Fig. 2. More than 80% of the background is from π^0 decay, directly from the Dalitz decay or indirectly from photon conversion. The π^0 spectrum is well constrained by the PHENIX measurement. The next most important background source is η decay. Given the assigned systematic error, the upper limit of the high p_T asymptotic η/π^0 ratio is 0.83. Since this ratio, corrected for feed-down, would imply that the primary $\eta/\pi^0 \sim 1$, this provides a conservative limit on contributions from η's. Contributions from all other hadrons combined are only a few percent of the total.

Background-subtracted electron spectra are shown in Fig. 3. The error bars on the data points represent the statistical errors, while the systematic error due to the background subtraction is indicated by brackets. The integrated yield of the electron signal dN_e/dy for $p_T > 0.8$ GeV/c is $0.025 \pm 0.004(\text{stat}) \pm 0.010(\text{syst})$ for central collisions and is $0.0079 \pm 0.0006(\text{stat}) \pm 0.0034(\text{syst})$ for minimum bias collisions.

Semileptonic decay of charmed hadrons is an expected source of the electron signal. We use the event generator PYTHIA [22] to estimate electron spectra from charm decay. We tuned the parameters [23] of PYTHIA such that charm production data at SPS and FNAL [24] and single electron data at the ISR [9–11] are well reproduced. The charm production cross section in pp collisions from this PYTHIA calculation is $\sigma_{c\bar{c}} = 330$ μb at $\sqrt{s} = 130$ GeV. The electron spectrum in Au + Au collisions is then calculated as $EdN_e/dp^3 = T_{AA} \times Ed\sigma_e/dp^3$, where $Ed\sigma_e/dp^3$ is the electron spectrum from charm decay calculated with PYTHIA, and T_{AA} (listed in Table I) is the nuclear overlap integral calculated from a Glauber model [13]. The calculated electron spectra shown in Fig. 3 are in reasonable agreement with the data.

Before attributing the entire electron signal to open charm decays, it is necessary to quantify contributions from other possible sources. An analogous PYTHIA estimate of the bottom decay contribution is shown in Fig. 3. It becomes significant only above the measured p_T range. Expected contributions from J/Ψ and Drell-Yan are negligible. In Pb + Pb collisions at SPS, direct photons [20] and an enhanced yield of low mass dileptons [25] have been reported. If these are due to thermal radiation from hot matter, an even larger production is expected at RHIC energies and can contribute to the electron signal. Since $\rho \rightarrow e^+e^-$ contributes less than 1% to the calculated background as shown in Fig. 2, and since the dominant
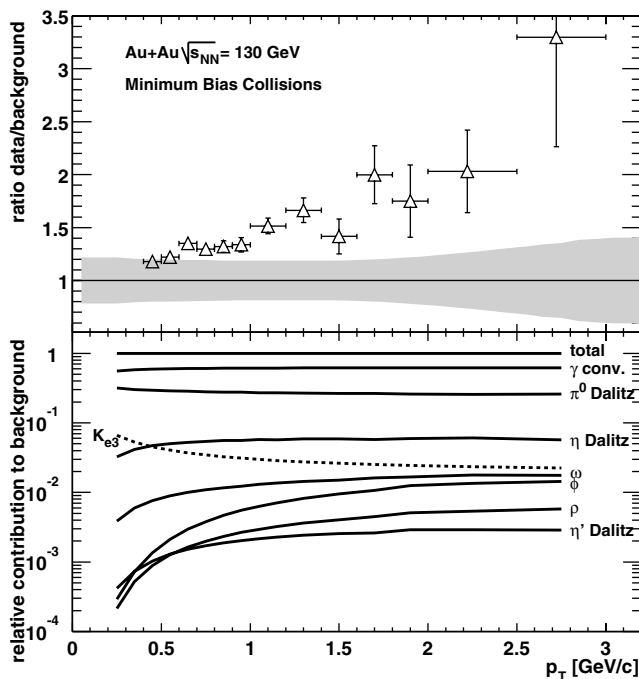

FIG. 2. Ratio of the electron data to the calculated background as a function of p_T in minimum bias collisions (upper panel) and relative contributions to the background from various sources (lower panel). The curves for ω and ϕ show the sum of the Dalitz and the dielectron decay modes.
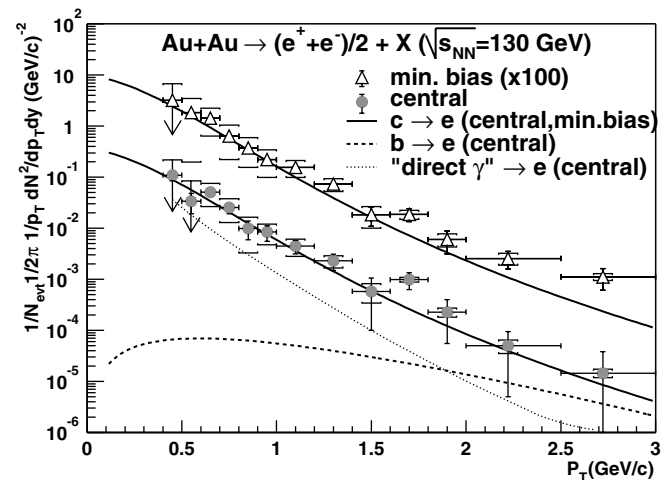

FIG. 3. The background-subtracted electron spectra for minimum bias (0%–92%) (scaled up by a factor of 100) and central (0%–10%) collisions compared with the expected contributions from open charm decays. Also shown, for central collisions only, are the expected contribution from bottom decays (dashed line) and the conversion electron spectrum from a direct photon prediction (dotted line).

TABLE I. Charm cross section per NN collision derived from the single electron data for central (0%–10%) and minimum bias (0%–92%) collisions. The first and second errors are statistical and systematic, respectively.

Centrality	T_{AA} (mb^{-1})	$d\sigma_{c\bar{c}}/dy|_{y=0}$ (μb)	$\sigma_{c\bar{c}}$ (μb)
0%–10%	22.6 ± 1.6(syst)	97 ± 13 ± 49	380 ± 60 ± 200
0%–92%	6.2 ± 0.4(syst)	107 ± 8 ± 63	420 ± 33 ± 250

source of thermal dileptons is $\pi + \pi \rightarrow \rho \rightarrow e^+ e^-$ [26], a significant contribution from thermal dileptons is unlikely. There are several predictions for direct photons at RHIC energies [27,28]. The conversion electron spectrum calculated from a prediction in Ref. [27] is shown in Fig. 3 for central collisions. It could explain 10%–20% of the signal, with large theoretical uncertainties.

Neglecting these other possible sources and assuming that all the electron signal is from charm, we derive the charm cross section corresponding to the electron data. We fit the charm electron spectrum from PYTHIA to the data for $p_T > 0.8$ GeV/c and obtain the rapidity density $dN_{c\bar{c}}/dy|_{y=0}$ and the total yield $N_{c\bar{c}}$ of open charm. They are then converted to cross sections per NN collision: $d\sigma_{c\bar{c}}/dy = (dN_{c\bar{c}}/dy)/T_{AA}$ and $\sigma_{c\bar{c}} = N_{c\bar{c}}/T_{AA}$. Results are shown in Table I. The systematic error is a quadratic sum of many sources. For central collisions, they are background subtraction ($\pm$44%), uncertainties in the PYTHIA calculation ($\pm$11% from $\langle k_T \rangle = 1.5 \pm 0.5$, $\pm$13% from $D^+/D^0 = 0.65 \pm 0.35$, $\pm$8% from PDFs), fit range ($\pm$18%), and T_{AA} ($\pm$7%). Note that any finite contribution from neglected sources would reduce the derived charm cross section. Without nuclear or medium effects in charm production, $\sigma_{c\bar{c}}$ per NN collision should be independent of centrality. Within uncertainties, our data

are consistent with this expectation, in possible contrast to the attribution of increased charm production as the source of enhanced dimuon production reported in Pb + Pb collisions at SPS [29].

The single electron signal yield (divided by T_{AA} to give the cross section per NN collision) and the derived charm cross section are compared with single electron data of ISR experiments and charm data of fixed target experiments [24] in Fig. 4. Cross section curves calculated with PYTHIA, which has been tuned to the charm data and the ISR electron data, and a charm cross section curve from a next-to-leading order (NLO) pQCD calculation [31] are also shown in the figure. Our data are consistent with both of the calculations within large uncertainties.

In conclusion, we have observed single electrons above the expected background from decays of light hadrons and photon conversion in Au + Au collisions at $\sqrt{s_{NN}} = 130$ GeV. The observed signal is consistent with semileptonic decay of charm. The forthcoming high statistics Au + Au data and pp comparison data at full RHIC energy ($\sqrt{s_{NN}} = 200$ GeV) will be useful to clarify the nature of the single electron signal and to better determine heavy-quark production in Au + Au collisions at RHIC.
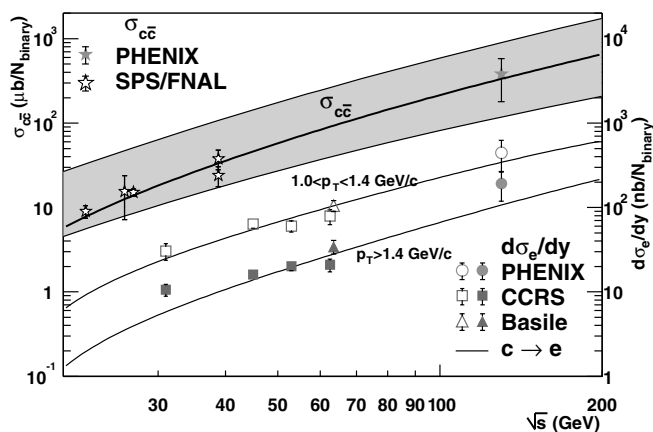
FIG. 4. Single electron cross sections $d\sigma_e/dy|_{y=0}$ of this measurement and ISR experiments [9,11,30] are displayed (bottom, right-hand scale) with charm decay contributions calculated with PYTHIA. Open and filled symbols are for $1.0 < p_T < 1.4$ GeV/c and $p_T > 1.4$ GeV/c, respectively. The derived charm cross section of this measurement is compared with charm cross sections from SPS/FNAL experiments (top, left-hand scale). The thick curve and the shaded band represent the charm cross section in the PYTHIA model and in a NLO pQCD calculation [31], respectively.

*Deceased.
†Not a participating institution.

[1] J. A. Appel, Annu. Rev. Nucl. Part. Sci. **42**, 367 (1992).
[2] B. Müller and X. N. Wang, Phys. Rev. Lett. **68**, 2437 (1992).
[3] Z. Lin and M. Gyulassy, Phys. Rev. Lett. **77**, 1222 (1996).
[4] Y. L. Dokshitzer and D. E. Kharzeev, Phys. Lett. B **519**, 199 (2001).
[5] T. Matsui and H. Satz, Phys. Lett. B **178**, 416 (1986).
[6] M. C. Abreu et al., Phys. Lett. B **447**, 28 (2000).
[7] R. Vogt et al., Phys. Rev. D **49**, 3345 (1994).
[8] F. W. Büsser et al., Phys. Lett. **53B**, 212 (1974).
[9] F. W. Büsser et al., Nucl. Phys. **B113**, 189 (1976).
[10] P. Perez et al., Phys. Lett. **112B**, 260 (1982).
[11] M. Basile et al., Nuovo Cimento Soc. Ital. Fis. **65A**, 421 (1981).

[12] I. Hinchliffe and C. H. Llewellyn Smith, Phys. Lett. **61B**, 472 (1976); M. Bourquin and J.-M. Gaillard, Nucl. Phys. **B114**, 334 (1976).

[13] K. Adcox *et al.,* Phys. Rev. Lett. **88**, 022301 (2002).

[14] H. Hamagaki *et al.,* Nucl. Phys. **A698**, 412 (2002).

[15] K. Adcox *et al.,* Phys. Rev. Lett. **86**, 3500 (2001).

[16] GEANT Users Guide, 3.15, CERN Program Library.

[17] K. Adcox *et al.,* nucl-ex/0112006.

[18] R. Albrecht *et al.,* Phys. Lett. B **361**, 14 (1995); G. Agakichiev *et al.,* Eur. Phys. J. C **4**, 249 (1998).

[19] M. Diakonou *et al.,* Phys. Lett. **89B**, 432 (1980).

[20] M. M. Aggarwal *et al.,* nucl-ex/0006007; M. M. Aggarwal *et al.,* Phys. Rev. Lett. **85**, 3595 (2000).

[21] C. Adler *et al.,* Phys. Rev. C **65**, R041901 (2002).

[22] T. Sjostrand, Comput. Phys. Commun. **82**, 74 (1994).

[23] We used PYTHIA 6.152 with CTEQ5L PDF [H. L. Lai *et al.,* Eur. Phys. J. C **12**, 375 (2000)]. Modified PYTHIA parameters are PARP(91) = 1.5 ($\langle k_t \rangle$), PMAS(4, 1) = 1.25 (m_c), PARP(31) = 3.5 (K factor), MSTP(33) = 1, MSTP(32) = 4 (Q^2 scale).

[24] G. A. Alves *et al.,* Phys. Rev. Lett. **77**, 2388 (1996).

[25] G. Agakichiev *et al.,* Phys. Lett. B **422**, 405 (1998).

[26] R. Rapp, Phys. Rev. C **63**, 054907 (2001).

[27] J. Alam *et al.,* Phys. Rev. C **63**, 021901 (2001).

[28] F. D. Steffen and M. H. Thoma, Phys. Lett. B **510**, 98 (2001); D. K. Srivastava, nucl-th/0103023.

[29] M. C. Abreu *et al.,* Eur. Phys. J. C **14**, 443 (2000).

[30] The $1.0 - 1.4$ GeV/c point of CCRS is calculated from the e/π ratio in Ref. [9] and the pion cross section in B. Alper *et al.,* Nucl. Phys. **B100**, 237 (1975).

[31] M. Mangano, P. Nason, and G. Ridolfi, Nucl. Phys. **B405**, 507 (1993). Their program HVQMNR is used with CTEQ5M PDF to calculate $\sigma_{c\bar{c}}$ in Fig. 4 with $m_c = 1.5$ GeV/c^2, $\mu_F = 2m_c$, and $0.5m_c < \mu_R < 2m_c$.